Am J Physiol Heart Circ Physiol 285: H283–H291, 2003;
10.1152/ajpheart.00954.2002.

Alterations in EDHF-type relaxation and phosphodiesterase activity in mesenteric arteries from diabetic rats

Takayuki Matsumoto, Tsuneo Kobayashi, and Katsuo Kamata
Department of Physiology and Morphology, Institute of Medicinal Chemistry, Hoshi University, Shinagawa-ku, Tokyo 142-8501, Japan

Submitted 5 November 2002; accepted in final form 19 March 2003

Matsumoto, Takayuki, Tsuneo Kobayashi, and Katsuo Kamata. Alterations in EDHF-type relaxation and phosphodiesterase activity in mesenteric arteries from diabetic rats. *Am J Physiol Heart Circ Physiol* 285: H283–H291, 2003; 10.1152/ajpheart.00954.2002.—In isolated superior mesenteric artery rings from age-matched control rats and streptozotocin (STZ)-induced diabetic rats, we investigated the role of cAMP in endothelium-derived hyperpolarizing factor (EDHF)-type relaxation. The ACh-induced EDHF-type relaxation was significantly weaker in STZ-induced diabetic rats than in control rats, and in both groups of rats it was attenuated by 18α-glycyrrhetinic acid (18α-GA), an inhibitor of gap junctions, and enhanced by IBMX, a cAMP-phosphodiesterase (PDE) inhibitor. These enhanced EDHF-type responses were very similar in magnitude between diabetic and age-matched control rats. The EDHF-type relaxation was enhanced by cilostamide, a PDE3-selective inhibitor, but not by Ro 20–1724, a PDE4-selective inhibitor. The expression levels of the mRNAs and proteins for two cAMP PDEs (PDE3A, PDE3B) were significantly increased in STZ-induced diabetic rats, but those for PDE4D were not. We conclude that the impairment of EDHF-type relaxations in STZ-induced diabetic rats may be attributed to a reduction in the action of cAMP via increased PDE activity.

endothelium-derived hyperpolarizing factor; adenosine 3′,5′-cyclic monophosphate; streptozotocin

THE ENDOTHELIUM PLAYS a major role in the regulation of vascular tone. It is capable of exerting a profound relaxing influence on the underlying smooth muscle, an effect mediated by at least three different factors, depending on the vascular bed. These factors include nitric oxide (NO) and prostacyclin, both diffusible factors (24, 31, 47, 52, 57). In addition, after blockade of NO and prostacyclin synthesis, stimulation of the endothelium is capable of evoking a vascular smooth muscle relaxation that has been attributed to a third factor, endothelium-derived hyperpolarizing factor (EDHF) (8, 21, 25, 67).

Although the identity of EDHF is still controversial (46), there is evidence that EDHF-type relaxations involve the transfer of a mediator from the endothelium to the smooth muscle via myoendothelial gap junctions (6, 20, 59). Indeed, EDHF-type responses are attenuated by connexin-mimetic peptides (6, 17, 30) and by 18α- and 18β-glycyrrhetinic acids (GA), aglycones that disrupt gap junction plaques at points of cell-to-cell contact (12, 66, 69).

It was recently reported that cAMP facilitates EDHF-type relaxation in conduit arteries by enhancing electrotonic conduction via gap junctions (26). In fact, EDHF-type relaxations are potentiated when cAMP hydrolysis is inhibited by the phosphodiesterase (PDE) inhibitor IBMX but remain susceptible to a combination of apamin plus charybdotoxin (65). In accord with such a role for gap junctions, the EDHF-type relaxations and cAMP accumulation evoked by ACh are inhibited by synthetic connexin-mimetic peptides, which interrupt intercellular communication in a connexin-specific fashion, and by 18α-GA (7, 27, 65).

The intracellular level of cAMP is dynamically regulated by the concerted actions of adenylyl cyclases and cyclic nucleotide PDE. To date, at least 11 distinct PDE families have been identified, in total containing more than 50 different PDE enzyme variants each encoded by several genes (3, 43, 62). In several animal species, an examination of the profiles of cAMP PDE activities in vascular smooth muscle cells (VSMCs) in contractile arteries identified PDE3 and PDE4 family members as being primarily responsible for cAMP PDE activity in these vessels (54). PDE3 is a high-affinity PDE (low-K_m cAMP PDE) that is sometimes referred to as cGMP-inhibited PDE (3, 44). Specific PDE3 inhibitors (e.g., cilostamide, milrinone, and lixazinone) promote smooth muscle relaxation, stimulate myocardial contractility, and inhibit platelet aggregation, suggesting an involvement of PDE3 in the regulation of these physiological processes (13, 28, 43). Molecular cloning studies revealed the presence of two distinct PDE3s, an adipocyte type (PDE3B) and a cardiac type (PDE3A) (14, 45, 61, 63). PDE3A mRNA is abundantly expressed in heart and vascular smooth muscle, whereas PDE3B mRNA is expressed in white and brown adipose tissue, hepatocytes, spermatocytes, and embryonic neuroepithelium, including the neural retina (58, 63). This tissue-specific distribution of PDE3A mRNA suggests the potential for PDE3A to be involved in diabetic vascular disease (48). Four PDE4 genes have

Address for reprint requests and other correspondence: K. Kamata, Dept. of Physiology and Morphology, Institute of Medicinal Chemistry, Hoshi Univ., Shinagawa-ku, Tokyo 142-8501, Japan (E-mail: kamata@hoshi.ac.jp).

The costs of publication of this article were defrayed in part by the payment of page charges. The article must therefore be hereby marked "*advertisement*" in accordance with 18 U.S.C. Section 1734 solely to indicate this fact.

been identified (*PDE4A*, *PDE4B*, *PDE4C*, and *PDE4D*), and PDE4 activity is detectable in most mammalian cells except blood platelets (11, 28). Perhaps because PDE4 inhibitors induce only weak vasorelaxations (54), the expression of PDE4s in blood vessels has not been studied extensively. Interestingly, it was reported recently that two PDE4D "long forms" (PDE4D3 and PDE4D5) are expressed in rat and human VSMCs (41, 51).

Diabetes mellitus is associated with vascular complications, including an impairment of vascular responsiveness to neurotransmitters in the macro- and microvasculature (15). In the former, there is an accumulating body of evidence to show that the relaxation responses induced in aortic strips by endothelium-dependent agents are weaker in streptozotocin (STZ)-induced diabetic rats than in nondiabetic control rats (10, 34, 37, 50, 53, 55). Recently, several reports indicated that an impairment of endothelium-dependent hyperpolarization and/or relaxation in the microvasculature can be induced by ACh in diabetic rats (23, 42, 68).

For the present study, we designed experiments to investigate the mechanisms underlying the diabetes-related impairment of ACh-induced endothelium-dependent vasodilation in the rat superior mesenteric artery. We were especially interested in cAMP-induced modulation of the EDHF-type relaxation in diabetes. We also asked whether mesenteric arteries from control and established diabetic rats might differ in their PDE expression profiles.

MATERIALS AND METHODS

Animals and Experimental Design

Male Wistar rats (8 wk old, 180- to 250-g body wt) received a single injection via the tail vein of 65 mg/kg STZ dissolved in a citrate buffer. Age-matched control rats were injected with the buffer alone. Food and water were given ad libitum. This study was conducted in accordance with the Guide for the Care and Use of Laboratory Animals adopted by the Committee on the Care and Use of Laboratory Animals of Hoshi University (which is accredited by the Ministry of Education, Science, Sports and Culture, Japan).

Measurement of Plasma Glucose

Twelve weeks after the injection of STZ or buffer, plasma glucose was determined with a commercially available enzyme kit (Wako Chemical, Osaka, Japan).

Measurement of Isometric Force

Rats were anesthetized with diethyl ether and euthanized by decapitation 12 wk after treatment with STZ or buffer. The superior mesenteric artery was rapidly removed and immersed in oxygenated, modified Krebs-Henseleit solution (KHS). This solution consisted of (in mM) 118.0 NaCl, 4.7 KCl, 25.0 $NaHCO_3$, 1.8 $CaCl_2$, 1.2 NaH_2PO_4, 1.2 $MgSO_4$, and 11.0 dextrose. The artery was carefully cleaned of all fat and connective tissue, and ring segments 2 mm in length were separately suspended by a pair of stainless steel pins in a well-oxygenated (95% O_2-5% CO_2) bath of 10 ml of KHS at 37°C. The rings were stretched until an optimal resting tension of 1.0 g was loaded and then allowed to equilibrate for at least 60 min. Force generation was monitored by means of an isometric transducer (model TB-611T; Nihon Kohden). The tissues were equilibrated for 40 min in the presence of 100 μM N^G-nitro-L-arginine (L-NNA) and 10 μM indomethacin to block nitric oxide synthase and cyclooxygenase, respectively, before administration of phenylephrine (1 μM). Once the phenylephrine-induced contraction was established, concentration-response curves were constructed for the relaxation induced by ACh or sodium nitroprusside (SNP). Such concentration-response curves were also generated in the combined presence of L-NNA (100 μM), indomethacin (10 μM), and one of 18α-GA, (100 μM for 40 min), IBMX (20 μM for 40 min), cilostamide (1 μM for 40 min), or Ro 20–1724 (10 μM for 40 min). In the experiments with IBMX and cilostamide, an equieffective concentration of phenylephrine was used (1–3 μM).

Enzyme Immunoassay for cAMP

Mesenteric rings from diabetic and age-matched control rats were incubated for 40 min at 37°C in oxygenated KHS containing L-NNA (100 μM) plus indomethacin (10 μM) with, in some experiments, cilostamide (1 μM) or Ro 20–1724 (10 μM). Phenylephrine (1 μM) was added 5 min before ACh stimulation. Rings were frozen in liquid N_2 after the addition of ACh (3 μM) and stored at −80°C. cAMP was subsequently extracted in 6% trichloroacetic acid, followed by neutralization with water-saturated diethyl ether and enzyme immunoassay (Amersham Biosciences UK).

Measurement of Expression of mRNAs for PDEs

Oligonucleotides. The primers used are summarized in Table 1.

RNA isolation and RT-PCR. RNA was isolated by the guanidinium method (9). Briefly, rat superior mesenteric arteries were carefully isolated and then cleaned of fat and connective tissue. The arteries were homogenized in RNA buffer, and the RNA was quantified by ultraviolet absorbance spectrophotometry. For the RT-PCR analysis, first-strand cDNA was synthesized from total RNA with oligo(dT) 12–18 and a cDNA synthesis kit (Life Sciences). Twenty (GAPDH), thirty (PDE3B), or twenty-seven (PDE4D) PCR cycles (94°C for 1 min, 54°C for 1 min, 72°C for 1 min) or twenty-six (PDE3A) PCR cycles (94°C for 1 min, 56°C for 1 min, 72°C for

Table 1. *PCR primers and PCR protocols*

cDNA (GenBank accession no.)	PCR Primer Sequences	PCR Protocols	Product Size, bp
GAPDH (X02231)	5′-TCCCTCAAGATTGTCAGCAA-3′ 5′-AGATCCACAACGGATACATT-3′	94°C/ 60 s 54°C/ 60 s 72°C/ 60 s 20 cycles	308
PDE3A (U38179)	5′-ATGTGGCCGTATTCTGAGC-3′ 5′-TACAGGGCCATCAACTCCA-3′	94°C/ 60 s 56°C/ 60 s 72°C/ 60 s 26 cycles	372
PDE3B (Z22867)	5′-TCTTTCACACCATTTCCTG-3′ 5′-CTGCTGCACTGGATACACT-3′	94°C/ 60 s 54°C/ 60 s 72°C/ 60 s 30 cycles	493
PDE4D (U09457)	5′-TGGTTGAAACGAAGAAGGT-3′ 5′-ACTCGCCATCTTCCTCTAA-3′	94°C/ 60 s 54°C/ 60 s 72°C/ 60 s 27 cycles	474

1 min) were performed with one-half of the reverse transcription mixture. The PCR products so obtained were analyzed on ethidium bromide-stained agarose (1.5%) gels. The PCR products were quantified by scanning densitometry, with the amount of each product being normalized with respect to the amount of GAPDH product.

Immunoprecipitation and Western Blotting

Snap-frozen mesenteric arterial tissues were homogenized in ice-cold lysis buffer containing 50 mM Tris·HCl (pH 7.5), 150 mM NaCl, 1% Triton X-100, and a protease-inhibitor cocktail. The protein concentration was determined by means of a bicinchoninic acid protein assay reagent kit (Pierce). Aliquot samples (200 μg) of tissue homogenates obtained from diabetic and age-matched control rats were then incubated with anti-PDE3A or anti-PDE3B antibody (Santa Cruz Biotechnology, Santa Cruz, CA; 1:100; 4°C, 4 h), followed by the addition of protein G Sepharose (Amersham Biosciences) for 2 h at 4°C. Immunoprecipitates were collected by centrifugation (13,000 *g*; 1 min), washed three times with buffer containing 50 mM Tris·HCl (pH 7.5), 150 mM NaCl, 0.1% Triton X-100, and a protease inhibitor cocktail, and resuspended in Laemmli's buffer containing mercaptoethanol. Samples were resolved by electrophoresis on 7.5% SDS-PAGE gels and transferred onto polyvinylidene difluoride membranes. Briefly, after the residual protein sites on the membrane were blocked with Block ace (Dainippon-pharm, Osaka, Japan), the membrane was incubated with anti-PDE3A or anti-PDE3B antibody (1:3,000) in blocking solution. Horseradish peroxidase-conjugated anti-goat antibody (Vector) was used at a 1:10,000 dilution in Tween-PBS, followed by detection with a SuperSignal (Pierce).

Drugs

Streptozotocin, phenylephrine, indomethacin, L-NNA, IBMX, 18α-GA, SNP, and protease inhibitor cocktail were all purchased from Sigma (St. Louis, MO). ACh chloride was from Daiichi Pharmaceuticals (Tokyo, Japan), and cilostamide and Ro 20–1724 were from Calbiochem-Novabiochem (La Jolla, CA) All drugs were dissolved in saline, except where otherwise noted. IBMX, 18α-GA, cilostamide, and Ro 20–1724 were dissolved in DMSO; control experiments confirmed the absence of significant effects on constrictor tone and ACh-induced relaxations at the final vehicle concentration used. All concentrations are expressed as the final molar concentration of the base in the organ bath.

Statistical Analysis

Data are expressed as means ± SE. When appropriate, statistical differences were assessed by Dunnett's test for multiple comparisons after a one-way ANOVA; a probability level of $P < 0.05$ was regarded as significant. Statistical comparisons between concentration-response curves were made by a two-way ANOVA, with Bonferroni's correction for multiple comparisons being performed post hoc ($P < 0.05$ again being considered significant).

RESULTS

Blood Glucose Levels and Animal Body Weights

At the time of the experiment, all STZ-treated rats exhibited hyperglycemia, their blood glucose concentrations (610.6 ± 29.6 mg/dl; $n = 12$) being significantly higher than those of the age-matched nondiabetic control rats (124.4 ± 3.4 mg/dl; $n = 12$). The body weights of the diabetic rats (236.3 ± 4.2 g; $n = 13$) were significantly lower than those of the age-matched control rats (472.6 ± 3.8 g; $n = 13$) at the time of the experiment.

ACh-Induced EDHF-Type Relaxation

To investigate the EDHF-type relaxation evoked by ACh in rat mesenteric artery, we performed a series of experiments in which ACh (10^{-9}–10^{-5} M) was added cumulatively to rings precontracted by phenylephrine (1 μM) in the presence of 100 μM L-NNA plus 10 μM indomethacin. The tension developed in response to 1 μM phenylephrine was 2.15 ± 0.86 g in diabetic mesenteric rings ($n = 13$) and 2.38 ± 0.7 g in those from the age-matched control rats ($n = 13$; no significant difference). The concentration-response curves for the peak amplitude of the EDHF-type relaxation induced by ACh in diabetic and age-matched control rats are shown in Fig. 1. The peak relaxation was significantly weaker in mesenteric arteries from diabetic rats [43.9 ± 3.9% and 69.3 ± 3.9% of the phenylephrine-induced tone in diabetic ($n = 13$) and age-matched control ($n = 13$) rats, respectively ($P < 0.001$)]. The EC_{50} values for the ACh-induced EDHF-type relaxations were 426.1 ± 99.0 and 65.1 ± 7.0 nM in diabetic and age-matched control rats, respectively ($P < 0.001$). Preparations incubated with 30 mM K^+ or denuded of their endothelium were essentially devoid of vasorelaxant activity (data not shown).

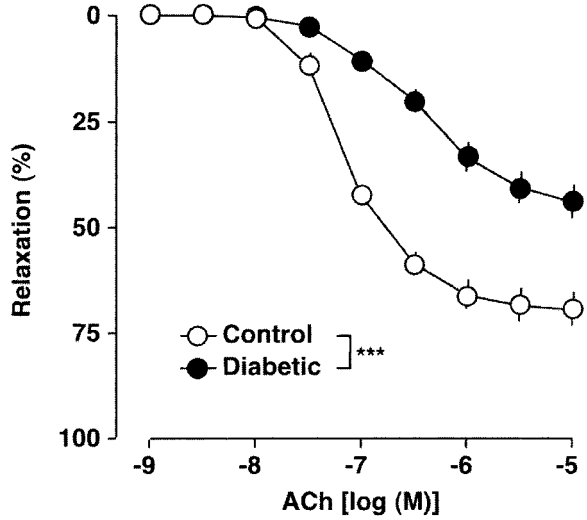

Fig. 1. Concentration-response curves for the endothelium-derived hyperpolarizing factor (EDHF)-type relaxations evoked by ACh in isolated rings of superior mesenteric artery obtained from age-matched control and diabetic rats. *y*-Axis shows relaxation of superior mesenteric artery as a percentage of the contraction induced by phenylephrine (1 μM). In each experiment, N^G-nitro-L-arginine (L-NNA; 100 μM) + indomethacin (10 μM) was applied 40 min before the phenylephrine application and was present thereafter. Each data point represents the mean ± SE from 13 experiments; the SE is included only when it exceeds the dimension of the symbol used. ***$P < 0.001$, diabetic vs. control.

Effect of 18α-GA on ACh-Induced EDHF-Type Relaxation

In several previous reports, gap junctional communication was said to contribute to the NO- and prostanoid-independent relaxations mediated via the endothelium (6, 12, 17, 20, 30, 66). To examine the part played by gap junctional communication in the present EDHF-type relaxation, rings were incubated with 18α-GA (12, 66, 69), a gap junction inhibitor (as well as with L-NNA + indomethacin) for 40 min before administration of phenylephrine. As shown in Fig. 2, ACh (10^{-9}–10^{-5} M) caused a reduced concentration-dependent relaxation in these rings whether they were from age-matched control rats or diabetic rats. This reduction was significant both for the age-matched control rats [Fig. 2*A*, maximal relaxation (R_{max}) = 16.3 ± 3.3, n = 6] and for the diabetic rats (Fig. 2*B*, R_{max} = 12.2 ± 2.0, n = 9). The present study confirmed that 18α-GA causes no significant alteration in SNP-induced relaxation (Fig. 2*C*) and has no significant effect on phenylephrine-induced contraction (data not shown).

Effect of PDE Inhibitors on ACh-Induced EDHF-Type Relaxation

Because PDE inhibitors have been shown to enhance the EDHF-type relaxation to ACh (7, 26, 65), we examined the effects of IBMX treatment on the present EDHF-type relaxation in diabetic and age-matched control rats. As IBMX depressed contraction, the concentration of phenylephrine used in experiments involving this agent was increased to between 1 and 3 μM. The tension developed in response to 1–3 μM phenylephrine in the presence of IBMX was 1.58 ± 0.05 g in diabetic mesenteric rings (n = 8) and 1.47 ± 0.06 g in age-matched control mesenteric rings (n = 8; no significant difference). The concentration-response curves for the peak amplitude of the EDHF-type relaxation induced by ACh in rings pretreated with IBMX are shown in Fig. 2. After incubation with 20 μM IBMX for 40 min, the R_{max} shown by rings from age-matched control rats was increased to 90.9 ± 2.5% with a leftward shift in the EC_{50} value to 52.0 ± 10.4 nM (Fig. 2*A*; n = 8) whereas in rings from diabetic rats the maximal relaxation was 91.7 ± 1.9% with a leftward shift in the EC_{50} value to 43.9 ± 9.4 nM (Fig. 2*B*; n = 8). There was no significant difference in the facilitated EDHF-type relaxation between diabetic and age-matched control rats.

Of the PDE families identified in VSMCs, members of the PDE3 (cGMP inhibited) and PDE4 (cAMP specific) families have been shown to contribute to the regulation of cAMP signaling and its impact on VSMC function (18, 51, 54). To investigate the effects of PDE-specific inhibitors on the present EDHF-type relaxation, we used cilostamide, a specific inhibitor of PDE3, and Ro 20–1724, a specific inhibitor of PDE4. When 1 μM cilostamide was added to rings (together with the usual L-NNA + indomethacin) for 40 min before administration of phenylephrine, there was no significant difference in the EDHF-type relaxation between rings

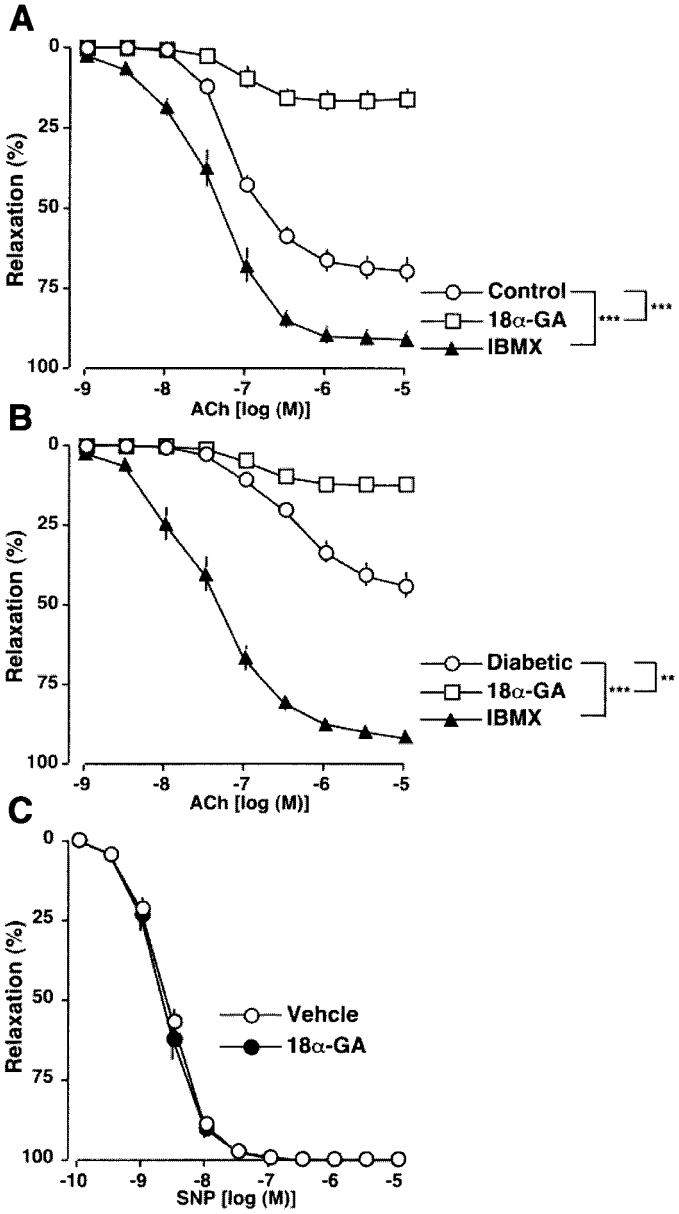

Fig. 2. Effects of the gap junction inhibitor 18α-glycyrrhetinic acid (18α-GA) and the cAMP phosphodiesterase (PDE) inhibitor IBMX on the EDHF-type relaxations evoked by ACh in superior mesenteric artery rings obtained from age-matched control (*A*) and diabetic (*B*) rats. In each experiment, L-NNA (100 μM) + indomethacin (10 μM) was applied 40 min before phenylephrine application and was present thereafter. ACh-induced relaxations [shown as % of phenylephrine (1 μM)-induced contraction] were attenuated by 18α-GA (100 μM for 40 min) with an associated rightward shift in the concentration-response curve. ACh-induced relaxations [shown as % of phenylephrine (1–3 μM)-induced contraction] were enhanced by IBMX (20 μM for 40 min) with an associated leftward shift in the concentration-response curve. Each data point represents the mean ± SE of ~6–9 experiments. ***P < 0.001, **P < 0.01, L-NNA + indomethacin group vs. L-NNA + indomethacin + 18α-GA or IBMX group. *C*: effect of 18α-GA on endothelium-independent relaxation in mesenteric artery obtained from control rats. Sodium nitroprusside (SNP)-induced vasodilation was not significantly different between vehicle (DMSO)- and 18α-GA-treated groups (n = 4).

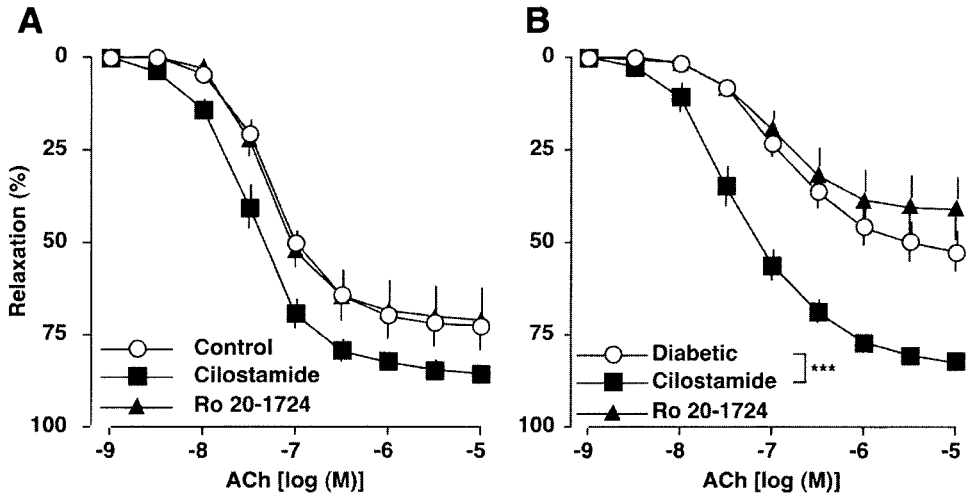

Fig. 3. Effects of specific cAMP-PDE inhibitors on the EDHF-type relaxations evoked by ACh in superior mesenteric artery rings obtained from age-matched control (*A*) and diabetic (*B*) rats. In each experiment, L-NNA (100 μM) + indomethacin (10 μM) was applied 40 min before phenylephrine application and was present thereafter. ACh-induced relaxations [shown as % of phenylephrine (1 μM)-induced contraction] were enhanced by the PDE3-selective inhibitor cilostamide (1 μM for 40 min) but not by the PDE4-selective inhibitor Ro 20–1724 (10 μM for 40 min), the former causing an associated leftward shift in the concentration-response curve. Each data point represents the mean ± SE from ~6–12 experiments. ***$P < 0.001$, L-NNA + indomethacin group vs. L-NNA + indomethacin + cilostamide group.

with cilostamide (R_{max} 85.4 ± 2.2%, EC_{50} 38.8 ± 5.7 nM; $n = 6$) and without (R_{max} 72.5 ± 4.4%, EC_{50} 61.8 ± 4.8 nM; $n = 7$) in age-matched control rats (Fig. 3*A*). However, the EDHF-type relaxation was significantly enhanced between rings with cilostamide (R_{max} 82.1 ± 2.1%, EC_{50} 55.2 ± 9.9 nM; $n = 11$) and without (R_{max} 52.4 ± 5.5%, EC_{50} 202.2 ± 48.8 nM; $n = 12$) in diabetic rats (Fig. 3*B*). In contrast, 10 μM Ro 20–1724 did not significantly alter the EDHF-type relaxation in rings from either diabetic (R_{max} 40.7 ± 8.6%, EC_{50} 137.8 ± 30.4 nM; $n = 11$) or age-matched control (R_{max} 70.8 ± 8.6%, EC_{50} 55.3 ± 4.3 nM; $n = 7$) rats.

cAMP Accumulation

cAMP levels were measured in rat mesenteric arterial rings treated with 100 μM L-NNA plus 10 μM indomethacin for 40 min (Fig. 4). Under our conditions, basal cAMP levels were not significantly different between diabetic and age-matched control rats. An ACh (3 μM)-induced cAMP accumulation was evident in both groups at 15 s, and these elevated cAMP levels were rapidly reduced (see 60 s ACh in Fig. 4). The extent of this decrease in cAMP levels (cAMP content at 15 s minus that at 60 s) was significantly larger in diabetic rats (4.868 ± 0.321 pmol/mg protein) than in control rats (2.274 ± 0.386 pmol/mg protein) ($P < 0.01$). Cilostamide (1 μM), but not Ro 20–1724 (10 μM), caused equivalent sustained increases in cAMP levels at 60 s in control and diabetic groups.

Expression of mRNAs and Proteins for PDEs

In vascular smooth muscle cells in several species, PDE3 and PDE4 family members are primarily responsible for cAMP-PDE activity in contractile arteries (54). As described above, PDE3 inhibition enhanced the EDHF-type relaxation to ACh in the diabetic mesenteric artery. To investigate the possible mechanisms underlying the impaired ACh-induced EDHF-type relaxation seen in STZ-induced diabetic rats, we examined whether the expressions of the mRNAs and pro-

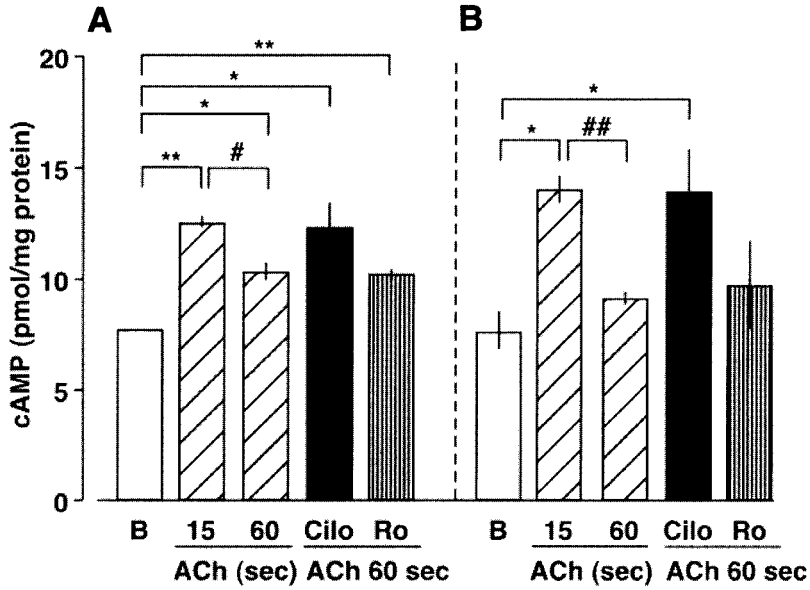

Fig. 4. cAMP levels in mesenteric arterial rings from control and diabetic rats. In endothelium-intact preparations incubated with L-NNA (100 μM) + indomethacin (10 μM) for 40 min, basal levels (B) before phenylephrine (1 μM) treatment were similar between control (*A*) and diabetic (*B*) groups. ACh (3 μM) induced a transient peak in cAMP levels in both control and diabetic groups. Cilostamide (1 μM; Cilo), but not Ro 20–1724 (Ro; 10 μM), caused equivalent sustained increases in cAMP levels in control and diabetic groups. Each column represents the mean ± SE from 3 experiments. *$P < 0.05$, **$P < 0.01$ vs. basal; #$P < 0.05$, ##$P < 0.01$, time 60 s vs. time 15 s.

teins for PDEs might be altered in the diabetic state. Using RT-PCR analysis on the total RNA isolated from superior mesenteric arteries from age-matched control and STZ-induced diabetic rats, we found that the expression of GAPDH mRNA showed no difference between the diabetic and age-matched control groups but the expressions of the mRNAs for PDE3A and PDE3B were significantly increased in the diabetic rats (compared with age-matched control rats). The expression of the mRNA for PDE4D, however, was not significantly increased (Fig. 5). Immunoblots of mesenteric arteries taken from diabetic and age-matched control rats and then treated with anti-PDE3A or anti-PDE3B antibody allowed detection of immunoreactive proteins with molecular masses of 120 and 135 kDa, respectively (Fig. 5*C*). PDE3A and PDE3B protein levels were increased in the diabetic rats compared with the age-matched control rats.

DISCUSSION

In the present study, we made two major findings concerning the impairment of EDHF-type relaxation in the mesenteric artery in STZ-induced diabetic rats and its modulation by cAMP.

Impaired endothelium-dependent relaxations have been consistently demonstrated in blood vessels from STZ-induced diabetic rats (15, 33, 34, 36, 37, 50). Although most studies of endothelial dysfunction in diabetes have focused on NO, an impairment of NO- and prostacyclin-resistant relaxation was recently reported in mesenteric arteries from diabetic rats (23, 42, 68). In the present study, our first finding was that the EDHF-type relaxation induced in the mesenteric artery by ACh was attenuated in STZ-induced diabetic rats (Fig. 1).

The identity of EDHF remains controversial (46). Recently, K^+ has been proposed as a candidate for EDHF in rat arteries (19). The postulated sequence would be that when ACh binds to muscarinic receptors on the endothelium, charybdotoxin- and apamin-sensitive K^+ channels in the endothelium are opened and K^+ efflux occurs in the myoendothelial space. The resulting increase in the myoendothelial K^+ concentration hyperpolarizes and relaxes adjacent smooth muscle cells by activating Ba^{2+}-sensitive K^+ channels and ouabain-sensitive Na^+-K^+-ATPase. However, there are other candidates for EDHF, namely endocannabinoids, anandamide, and epoxyeicosatrienoic acids, which are cytochrome *P*-450-monooxygenase-derived metabolites of arachidonic acid (5, 22, 29, 46, 56). Furthermore, recent evidence suggests that direct heterocellular gap junctional communication between endothelial and smooth muscle cells may contribute to NO-independent relaxation (6, 20, 30, 66, 69). In the present study, we demonstrated that in the rat superior mesenteric artery, ACh-induced EDHF-type relaxation is mediated via gap junctions (because the relaxation was largely blocked by pretreatment with 18α-GA; Fig. 2).

Gap junctional communication plays an important role in vascular tissue homeostasis. The hallmark of the vasorelaxation attributed to EDHF is that it is accompanied by membrane hyperpolarization. The hyperpolarization generated in endothelial cells is capable of spreading electrotonically to the underlying smooth muscle cells, most likely via myoendothelial gap junctions. Evidence supporting the transfer of a small molecule (e.g., cAMP) via myoendothelial gap junctions has also been presented. Recently, in culture experiments, it was reported that high glucose reduced

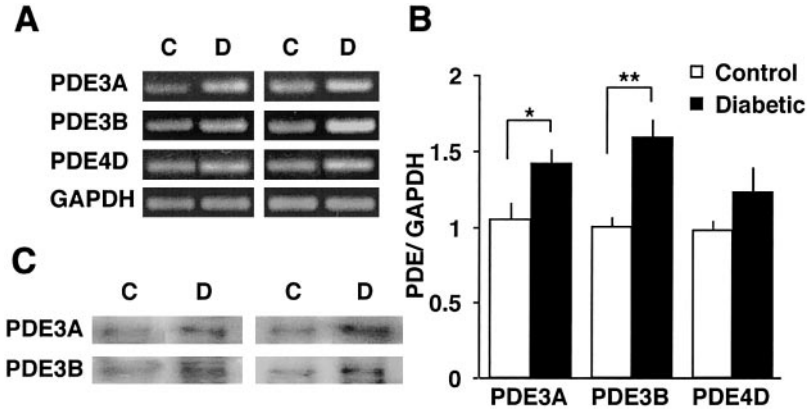

Fig. 5. RT-PCR assay of expressions of the mRNAs for PDEs and immunoblot analysis of protein levels in superior mesenteric arteries from control and diabetic rats. *A*: expression of the mRNAs for PDE3A, PDE3B, and PDE4D in control (C) and diabetic (D) rat mesenteric arteries, as assayed by RT-PCR. *B*: quantitative analysis of the expressions of the mRNAs for PDEs by scanning densitometry. Values are means ± SE of 3 determinations (PDE/GAPDH); control rats: $n = 3$, STZ-induced diabetic rats: $n = 3$. $^*P < 0.05$, $^{**}P < 0.01$, diabetic vs. control. The RT-PCR assay was performed as described in MATERIALS AND METHODS. Each total RNA preparation (3.0 μg) was reverse-transcribed, and one-half of the cDNA product was PCR-amplified with various primers, several cycles being used. A portion of the PCR reaction product was electrophoresed on a 1.5% agarose gel containing ethidium bromide. *C*: immunoblots showing protein expressions of PDE3A (120 kDa) and PDE3B (135 kDa) in rat mesenteric arteries obtained from age-matched control and diabetic rats. Two examples are shown for each PDE. Details are given in MATERIALS AND METHODS.

gap junction activity (38, 60). Although our data demonstrated that the present EDHF-type relaxation was mediated by gap junctions, it remains to be determined in future studies whether gap junction activity is directly impaired in STZ-induced diabetic rats.

Recent studies reported that cAMP facilitates EDHF-type relaxations in conduit arteries via gap junctional communication (7, 26, 27, 65). Experiments with the P site agonist 2′,3′-dideoxyadenosine (2′,3′-DDA) and forskolin, which respectively inhibit and stimulate adenylate cyclase (16, 32, 39), also provided insights into the cellular mechanisms that underlie the EDHF phenomenon by demonstrating a central role for cAMP. In our previous studies (35) we observed an NO-independent decrease in the forskolin-induced relaxation after endothelial denudation in the rat mesenteric bed, and others (40) reported that the IC_{50} value for the cAMP accumulation induced by this agent is shifted approximately threefold to the right after endothelial denudation in rabbit arteries. It was also demonstrated that the endothelium is a major source of cAMP. For example, in the perfused rat mesentery the extracellular release of cAMP in response to ACh or the Ca^{2+}-ATPase inhibitor cyclopiazonic acid, both of which evoke EDHF-type relaxations sensitive to Gap 27 peptide and 18α-GA (6, 17, 30, 66), is markedly reduced by endothelial denudation (1, 35). Having found that the EDHF-type relaxations in our preparations were mediated by gap junctions, we examined the effects of cAMP PDE inhibitors on EDHF-type relaxation (Fig. 2). This relaxation in the rat superior mesenteric artery was potentiated in the presence of IBMX, and this potentiation was larger in diabetic rats than in control rats (with the result that in IBMX-treated rings, the EDHF-type relaxations were very similar between control and diabetic rats). These findings suggest that cAMP signaling is impaired in the diabetic state. Indeed, in our previous study (2), the ACh-induced cAMP release from a mesentery preparation was decreased in the diabetic rat group.

cAMP signaling in mammalian cells is terminated by cyclic nucleotide PDEs, a multifamily class of enzymes that catalyze the hydrolysis of cyclic nucleotides to 5′-nucleotide monophosphates (which do not activate cAMP effector proteins; Refs. 3, 4). Among the various PDEs, PDE3 and PDE4 are of most interest because they preferentially hydrolyze cAMP (54). It was reported recently that PDE3 and PDE4 activities are altered in diabetes (48, 49). Nagaoka et al. (48) reported that the increased PDE3 activity in the aorta of atherosclerosis-prone insulin-resistant cp/cp rats correlated positively with an increased amount of PDE3A mRNA. Also, Tang et al. (64) reported that in adipose tissue of obese insulin-resistant diabetic KKAy mice, PDE3B mRNA and its corresponding protein were reduced to 48 and 43%, respectively, of those in C57BL/6J control mice. Basal and insulin-stimulated membrane-bound PDE activities were also decreased to 50 and 36%, respectively, of those in the control rats. Pioglitazone increased both PDE3B mRNA and protein levels by 1.8-fold those in untreated KKAy mice. Basal and insulin-induced membrane-bound PDE activities were also increased by 1.6- and 2.0-fold, respectively. This study also suggested that mRNA and protein for PDE3 were correlated with changes in PDE3 activities. We found in the present study that when ACh was applied to mesenteric arteries, the cAMP level was significantly lower at 60 s than at 15 s, and this decrease was significantly greater in the diabetic state than in the control state (Fig. 4). These data are consistent with the increased expressions of PDE3, but not PDE4, mRNA, and protein levels in diabetic rats (Fig. 5). Together, the present results suggest that PDE3 activities are increased in STZ-induced diabetic rats. In line with this, we found that, although the ACh-induced EDHF-type relaxation was impaired in diabetic rats, the cilostamide-induced enhancement of EDHF-type relaxation was greater in diabetic rats than in control rats (Fig. 3). On the other hand, our data suggest that PDE4 may not contribute to the present EDHF-type relaxation because Ro 20–1724 was without effect.

In conclusion, we found *1*) that cAMP and gap junctional communication play important roles in EDHF-type relaxation in rat mesenteric artery and *2*) that the impaired EDHF-type relaxation in the mesenteric artery that we saw in STZ-induced diabetic rats may be attributed to a reduced action of cAMP, in turn resulting from increased PDE3 activity. We believe that our findings should stimulate further interest in PDE3 as a potential therapeutic target in the continuing efforts to reduce diabetes-associated vascular disease.

We thank K. Taguchi and K. Wakabayashi for technical help.

This study was supported in part by the Ministry of Education, Science, Sports and Culture, Japan.

REFERENCES

1. **Abiru T, Watanabe Y, Kamata K, and Kasuya Y.** Simultaneous measurement of vasodilation and changes in cyclic nucleotides in the perfused mesenteric arterial bed of the rat. *Eur J Pharmacol* 242: 15–22, 1993.
2. **Abiru T, Watanabe Y, Kamata K, and Kasuya Y.** Changes in endothelium-dependent relaxation and levels of cyclic nucleotides in the perfused mesenteric arterial bed from streptozotocin-induced diabetic rats. *Life Sci* 53: PL7–PL12, 1993.
3. **Beavo JA.** Cyclic nucleotide phosphodiesterases: functional implications of multiple isoforms. *Physiol Rev* 75: 725–748, 1995.
4. **Beavo JA and Reifsnyder DH.** Primary sequence of cyclic nucleotide phosphodiesterase isozymes and the design of selective inhibitors. *Trends Pharmacol Sci* 11: 150–155, 1990.
5. **Campbell WB, Gebremedhin D, Pratt PF, and Harder DR.** Identification of epoxyeicosatrienoic acids as endothelium-derived hyperpolarizing factors. *Circ Res* 78: 415–423, 1996.
6. **Chaytor AT, Evans WH, and Griffith TM.** Central role of heterocellular gap junctional communication in endothelium-dependent relaxations of rabbit arteries. *J Physiol* 508: 561–573, 1998.
7. **Chaytor AT, Taylor HJ, and Griffith TM.** Gap junction-dependent and -independent EDHF-type relaxations may involve smooth muscle cAMP accumulation. *Am J Physiol Heart Circ Physiol* 282: H1548–H1555, 2002.
8. **Chen G, Suzuki H, and Weston AH.** Acetylcholine releases endothelium-derived hyperpolarizing factor and EDRF from rat blood vessels. *Br J Pharmacol* 95: 1165–1174, 1988.
9. **Chomczynski P and Sacchi N.** Single-step method of RNA isolation by acid guanidinium thiocyanate-phenol-chloroform extraction. *Anal Biochem* 162: 156–159, 1987.

10. **Cohen RA.** The role of nitric oxide and other endothelium-derived vasoactive substances in vascular disease. *Prog Cardiovasc Dis* 38: 105–128, 1995.
11. **Conti M and Jin SL.** The molecular biology of cyclic nucleotide phosphodiesterases. *Prog Nucleic Acid Res Mol Biol* 63: 1–38, 1999.
12. **Davidson JS, Baumgarten IM, and Hartley EH.** Reversible inhibition of intracellular junctional communication by glycyrrhetinic acid. *Biochem Biophys Res Commun* 134: 29–36, 1986.
13. **Degerman E, Belfrage P, and Manganiello VC.** cGMP-inhibited phosphodiesterases (PDE3 gene family). *Biochem Soc Trans* 24: 1010–1014, 1996.
14. **Degerman E, Belfrage P, and Manganiello VC.** Structure, localization, and regulation of cGMP-inhibited phosphodiesterase (PDE3). *J Biol Chem* 272: 6823–6826, 1997.
15. **De Vriese AS, Verbeuren TJ, Van de Voorde J, Lamiere NH, and Vanhoutte PM.** Endothelial dysfunction in diabetes. *Br J Pharmacol* 130: 963–974, 2000.
16. **Dong H, Waldron GJ, Cole WC, and Triggle CR.** Role of calcium-activated and voltage-gated delayed rectifier potassium channels in endothelium-dependent vasorelaxation of the rabbit middle cerebral artery. *Br J Pharmacol* 123: 821–832, 1998.
17. **Dora KA, Martin PEM, Chaytor AT, Evans WH, Garland CJ, and Griffith TM.** Role of heterocellular gap junctional communication in endothelium-dependent smooth muscle hyperpolarization: inhibition by a connexin-mimetic peptide. *Biochem Biophys Res Commun* 254: 27–31, 1999.
18. **Douglas GT and Maurice DH.** Vascular smooth muscle cell phosphodiesterase (PDE)3 and PDE4 activities and levels are regulated by cyclic AMP in vivo. *Mol Pharmacol* 62: 497–506, 2002.
19. **Edwards G, Dora KA, Gardener MJ, Garland CJ, and Weston AH.** K^+ is an endothelium-derived hyperpolarizing factor in rat arteries. *Nature* 396: 269–272, 1998.
20. **Edwards G, Feletou M, Gardener MJ, Thollon C, Vanhoutte PM, and Weston AH.** Role of gap junctions in the responses to EDHF in rat and guinea-pig small arteries. *Br J Pharmacol* 128: 1788–1794, 1999.
21. **Feletou M and Vanhoutte PM.** Endothelium-dependent hyperpolarization of canine coronary smooth muscle. *Br J Pharmacol* 93: 515–524, 1988.
22. **Fisslthaler B, Popp R, Kiss L, Potente M, Harder DR, Fleming I, and Busse R.** Cytochrome P450 2C is an EDHF synthase in coronary arteries. *Nature* 401: 493–497, 1999.
23. **Fukao M, Hattori Y, Kanno M, Sakuma I, and Kitabatake A.** Alterations in endothelium-dependent hyperpolarization and relaxation in mesenteric arteries from streptozotocin-induced diabetic rats. *Br J Pharmacol* 121: 1383–1391, 1997.
24. **Furchgott RF and Zadwadzki JV.** The obligatory role of endothelial cells in the relaxation of arterial smooth muscle by acetylcholine. *Nature* 288: 373–376, 1980.
25. **Garland CJ, Plane F, Kemp BK, and Cocks TM.** Endothelium-dependent hyperpolarization: a role in the control of vascular tone. *Trends Pharmacol Sci* 16: 23–30, 1995.
26. **Griffith TM, Chaytor AT, Taylor HJ, Giddings BD, and Edwards DH.** cAMP facilitates EDHF-type relaxations in conduit arteries by enhancing electronic conduction via gap junctions. *Proc Natl Acad Sci USA* 99: 6392–6397, 2002.
27. **Griffith TM and Taylor HJ.** Cyclic AMP mediates EDHF-type relaxations of rabbit jugular vein. *Biochem Biophys Res Commun* 263: 52–57, 1999.
28. **Haslam RJ, Dickinson NT, and Jang EK.** Cyclic nucleotides and phosphodiesterases in platelets. *Thromb Haemost* 82: 412–423, 1999.
29. **Hecker M, Bara AT, Bauersachs J, and Busse R.** Characterization of endothelium-derived hyperpolarizing factor as a cytochrome p450-derived arachidonic acid metabolite in mammals. *J Physiol* 481: 407–414, 1994.
30. **Hutcheson IR, Chaytor AT, Evans EH, and Griffith TM.** Nitric oxide-independent relaxations to acetylcholine and A23187 involve different routes of heterocellular communication. *Circ Res* 84: 53–63, 1999.
31. **Ignarro LJ, Buga GM, Wood KS, Byrns RE, and Chaudhuri G.** Endothelium-derived relaxing factor produced and released from artery and vein is nitric oxide. *Proc Natl Acad Sci USA* 84: 9265–9269, 1987.
32. **Johnson RA and Shoshani I.** Kinetics of "P"-site-mediated inhibition of adenylyl cyclase and the requirements for substrate. *J Biol Chem* 265: 11595–11600, 1990.
33. **Kamata K and Kobayashi T.** Changes in superoxide dismutase mRNA expression by streptozotocin-induced diabetes. *Br J Pharmacol* 119: 583–589, 1996.
34. **Kamata K, Miyata N, and Kasuya Y.** Impairment of endothelium-dependent relaxation and changes in levels of cyclic GMP in aorta from streptozotocin-induced diabetic rats. *Br J Pharmacol* 97: 614–618, 1989.
35. **Kamata K, Umeda F, and Kasuya Y.** Possible existence of novel endothelium-derived relaxing factor in the endothelium of rat mesenteric arterial bed. *J Cardiovasc Pharmacol* 27: 601–606, 1996.
36. **Kobayashi T and Kamata K.** Relationship among cholesterol, superoxide anion and endothelium-dependent relaxation in diabetic rats. *Eur J Pharmacol* 367: 213–222, 1999.
37. **Kobayashi T, Matsumoto T, and Kamata K.** Mechanisms underlying the chronic pravastatin treatment-induced improvement in the impaired endothelium-dependent aortic relaxation seen in streptozotocin-induced diabetic rats. *Br J Pharmacol* 131: 231–238, 2000.
38. **Kuroki T, Inoguchi T, Umeda F, Ueda F, and Nawata H.** High glucose induces alteration of gap junction permeability and phosphorylation of connexin-43 in cultured aortic smooth muscle cells. *Diabetes* 47: 931–936, 1998.
39. **Legrand AB, Narayanan TK, Ryan US, Aronstam RS, and Catravas JD.** Modulation of adenylate cyclase activity in cultured bovine pulmonary arterial endothelial cells. Effects of adenosine and derivatives. *Biochem Pharmacol* 38: 423–430, 1989.
40. **Linz W, Wiemer G, and Scholkens BA.** Effects of colforsin, trequinsin and isoprenaline on norepinephrine-induced contractions and cyclic nucleotide levels of isolated vascular tissue. *Arzneimittelforschung* 38: 240–243, 1988.
41. **Liu H and Maurice DH.** Phosphorylation-mediated activation and translocation of the cyclic AMP-specific phosphodiesterase PDE4D3 by cyclic AMP-dependent protein kinase and mitogen-activated protein kinases. A potential mechanism allowing for the coordinated regulation of PDE4D activity and targeting. *J Biol Chem* 274: 10557–10565, 1999.
42. **Makino A, Ohuchi K, and Kamata K.** Mechanisms underlying the attenuation of endothelium-dependent vasodilatation in the mesenteric arterial bed of the streptozotocin-induced diabetic rat. *Br J Pharmacol* 130: 549–556, 2000.
43. **Manganiello VC and Degerman E.** Cyclic nucleotide phosphodiesterases (PDEs): diverse regulators of cyclic nucleotide signals and inviting molecular targets for novel therapeutic agents. *Thromb Haemost* 82: 407–411, 1999.
44. **Manganiello VC, Murata T, Taira T, Belfrage P, and Degerman E.** Diversity in cyclic nucleotide phosphodiesterase isoenzyme families. *Arch Biochem Biophys* 322: 1–13, 1995.
45. **Meacci E, Taira M, Moos M Jr, Smith CJ, Movsesian MA, Degerman E, Belfrage P, and Manganiello VC.** Molecular cloning and expression of human myocardial cGMP-inhibited cAMP phosphodiesterase. *Proc Natl Acad Sci USA* 89: 3721–3725, 1992.
46. **Mombouli JV and Vanhoutte PM.** Endothelium-derived hyperpolarizing factor(s): updating the unknown. *Trends Pharmacol Sci* 18: 252–256, 1997.
47. **Moncada S, Gryglewski R, Bunting S, and Vane JR.** An enzyme isolated from arteries transforms prostaglandin endoperoxides to an unstable substance that inhibits platelet aggregation. *Nature* 263: 663–665, 1976.
48. **Nagaoka T, Shirakawa T, Balon TW, Russel JC, and Fujita-Yamaguchi Y.** Cyclic nucleotide phosphodiesterase 3 expression in vivo: evidence for tissue-specific expression of phosphodiesterase 3A or 3B mRNA and activity in the aorta and adipose tissue of atherosclerosis-prone insulin-resistant rats. *Diabetes* 47: 1135–1144, 1998.
49. **Netherton SJ, Jimmo SL, Palmer D, Tilley DG, Dunkerley HA, Raymond DR, Russell JC, Absher M, Sage EH, Vernon**

RB, and Maurice DH. Altered phosphodiesterase 3-mediated cAMP hydrolysis contributes to a hypermotile phenotype in obese JCR:LA-cp rat aortic vascular smooth muscle cells: implications for diabetes-associated cardiovascular disease. *Diabetes* 51: 1194–1200, 2002.

50. **Oyama Y, Kawasaki H, Hattori Y, and Kanno M.** Attenuation of endothelium-dependent relaxation in aorta from diabetic rats. *Eur J Pharmacol* 132: 75–78, 1986.
51. **Palmer D and Maurice DH.** Dual expression and difference regulation of phosphodiesterase 3A and phosphodiesterase 3B in human vascular smooth muscle: implications for phosphodiesterase 3 inhibition in human cardiovascular tissues. *Mol Pharmacol* 58: 247–252, 2000.
52. **Palmer RM, Ashton DS, and Moncada S.** Vascular endothelial cells synthesize nitric oxide from L-arginine. *Nature* 333: 664–666, 1988.
53. **Pieper GM.** Review of alterations in endothelial nitric oxide production in diabetes: protective role of arginine on endothelial dysfunction. *Hypertension* 31: 1047–1060, 1998.
54. **Polson JB and Strada SJ.** Cyclic nucleotide phosphodiesterases and vascular smooth muscle. *Annu Rev Pharmacol Toxicol* 36: 403–427, 1996.
55. **Poston L and Taylor PD.** Endothelial-mediated vascular function in insulin-dependent diabetes mellitus. *Clin Sci (Lond)* 88: 245–255, 1995.
56. **Randall MD and Kendall DA.** Endocannabinoids: a new class of vasoactive substances. *Trends Pharmacol Sci* 19: 55–58, 1998.
57. **Rapoport RM and Murad F.** Agonist-induced endothelium-dependent relaxation in rat thoracic aorta may be mediated through cGMP. *Circ Res* 52: 352–357, 1983.
58. **Reinhardt RR, Chin E, Zhou J, Taira M, Murata T, Manganiello VC, and Bondy CA.** Distinctive anatomical patterns of gene expression for two cGMP-inhibited cyclic nucleotide phosphodiesterase subfamilies. *J Clin Invest* 95: 1528–1538, 1995.
59. **Sandow SL, Tare M, Coleman HA, Hill CE, and Parkington HC.** Involvement of myoendothelial gap junctions in the actions of endothelium-derived hyperpolarizing factor. *Circ Res* 90: 1108–1113, 2002.
60. **Sato T, Haimovici R, Kao R, Li AF, and Roy S.** Downregulation of connexin 43 expression by high glucose reduces gap junction activity in microvascular endothelial cells. *Diabetes* 51: 1565–1571, 2002.
61. **Smith CJ, Huang R, Sun D, Ricketts S, Hoegler C, Ding JZ, Moggio RA, and Hintze TH.** Development of decompensated dilated cardiomyopathy is associated with decreased gene expression and activity of the milrinone-sensitive cAMP phosphodiesterase PDE3A. *Circulation* 96: 3116–3123, 1997.
62. **Soderling SH and Beavo JA.** Regulation of cAMP and cGMP signaling: new phosphodiesterase and new functions. *Curr Opin Cell Biol* 12: 174–179, 2000.
63. **Taira M, Hockman SC, Calvo JC, Taira M, Belfrage P, and Manganiello VC.** Molecular cloning of the rat adipocyte hormone-sensitive cyclic GMP-inhibited cyclic nucleotide phosphodiesterase. *J Biol Chem* 268: 18573–18579, 1993.
64. **Tang Y, Osawa H, Onuma H, Nishimiya T, Ochi M, and Makino H.** Improvement in insulin resistance and the restoration of reduced phosphodiesterase 3B gene expression by pioglitazone in adipose tissue of obese diabetic KKAy mice. *Diabetes* 48: 1830–1835, 1999.
65. **Taylor HJ, Chaytor AT, Edwards DH, and Griffith TM.** Gap junction-dependent increases in smooth muscle cAMP underpin the EDHF phenomenon in rabbit arteries. *Biochem Biophys Res Commun* 283: 583–589, 2001.
66. **Taylor HJ, Chaytor AT, Evans WH, and Griffith TM.** Inhibition of gap junctional component of endothelium-dependent relaxations in rabbit iliac artery by 18α-glycyrrhetinic acid. *Br J Pharmacol* 125: 1–3, 1998.
67. **Taylor SG and Weston AH.** Endothelium-derived hyperpolarizing factor: a new endogenous inhibitor from the vascular endothelium. *Trends Pharmacol Sci* 9: 272–274, 1988.
68. **Wigg SJ, Tare M, Tonta MA, O'brien RC, Meredith IT, and Parkington HC.** Comparison of effects of diabetes mellitus on an EDHF-dependent and an EDHF-independent artery. *Am J Physiol Heart Circ Physiol* 281: H232–H240, 2001.
69. **Yamamoto Y, Imaeda K, and Suzuki H.** Endothelium-dependent hyperpolarization and intercellular electrical coupling in guinea-pig mesenteric arterioles. *J Physiol* 514: 505–513, 1999.